



University
of Glasgow

Merrifield, G. D., Brydges, N. M., Hall, L., Mullin, J., Gallagher, L., Pizzi, R. and Holmes, W. M. (2018) Measures of cardiac function in Theraphosidae spiders using in vivo magnetic resonance imaging. *Physiological Entomology*, 43(3), pp. 207-213. (doi:[10.1111/phen.12245](https://doi.org/10.1111/phen.12245)).

There may be differences between this version and the published version. You are advised to consult the publisher's version if you wish to cite from it.

This is the peer reviewed version of the following article: Merrifield, G. D., Brydges, N. M., Hall, L., Mullin, J., Gallagher, L., Pizzi, R. and Holmes, W. M. (2018) Measures of cardiac function in Theraphosidae spiders using in vivo magnetic resonance imaging. *Physiological Entomology*, 43(3), pp. 207-213, which has been published in final form at [10.1111/phen.12245](https://doi.org/10.1111/phen.12245). This article may be used for non-commercial purposes in accordance with [Wiley Terms and Conditions for Self-Archiving](#).

<http://eprints.gla.ac.uk/162275/>

Deposited on: 14 May 2018

1 **Measures of Cardiac Function in Theraphosidae Spiders using *in vivo***
2 **Magnetic Resonance Imaging**

3
4 **Authors**

5 Gavin D. Merrifield* (1)

6 Nichola M. Brydges (2)

7 Lynsey Hall (3)

8 James Mullin (1)

9 Lindsay Gallagher (1)

10 Romain Pizzi (4, 5)

11 William M. Holmes (1)

12 **Addresses:**

13 1. Glasgow Experimental Magnetic Resonance Imaging Centre, College of
14 Medical, Veterinary and Life Sciences, University of Glasgow, Glasgow, UK

15 2. Institute of Psychological Medicine and Clinical Neurosciences, Cardiff
16 University School of Medicine, Cardiff, UK

17 3. University of Newcastle, Newcastle, UK

18 4. Royal Zoological Society of Scotland, UK

19 5. School of Veterinary Medicine and Science, University of Nottingham, UK

20
21 *Corresponding Author

22 g.d.merrifield@gmail.com

23
24 **Keywords**

25 MRI, cardiac function, Theraphosidae, tarantula, ejection fraction, *in vivo*, magnetic
26 resonance, heart rate

27
28
29

30

31 **Abstract**

32

33 We present the first *in vivo* cardiac Magnetic Resonance Imaging (MRI)
34 measurements of Theraphosidae spiders. MRI scanning was performed on six
35 spiders under isoflurane-induced anaesthesia. Retrospective Self-Gating Cine-
36 Cardiac MRI (RG-CINE-MRI) was used to overcome the difficulties of prospective
37 cardiac gating in this species. The resulting RG-CINE-MRI images were successfully
38 analysed to obtain functional cardiac parameters from live spiders at rest. Cardiac
39 ejection fraction was found to increase with animal mass (Pearson correlation 0.849,
40 $p= 0.03$) at a faster rate than myocardial tissue volume, while heart rate stayed
41 constant across animals. Suggesting the spider heart undergoes additional
42 biomechanical loading with age. The acquisition of these results demonstrates the
43 potential for retrospective gating to evaluate aspects of cardiac function in a wide
44 range of previously inaccessible species.

45

46

47 **Introduction**

48

49 To date, the cardiac physiology of invertebrates in general, and spiders in particular,
50 has been comparatively little studied next to the great volume of cardiac literature
51 amassed for rodents and humans, particularly in the medical sciences. Additionally
52 for spiders the techniques used have been restricted to measurements of heart
53 action potential via electrocardiogram (ECG) (Dunlop et al.,1992) or monitoring
54 exterior cuticle movement as a proxy for cardiac motion (Bromhall, 1987; Coelho and
55 Amaya 2000) . These latter observations have included both visual observation and
56 the use of attached magnets and sensors to gauge movement. Many of these
57 methods involve either attaching experimental apparatus to the animal, penetrating
58 the outer cuticle (which could potentially lead to lowering of the internal
59 hydrodynamic pressure) or indirect observations of heart function. Therefore, there
60 is little quantitative information on spider cardiac function and outputs in the
61 literature.

62

63 This is in contrast to many vertebrates where cardiovascular Magnetic Resonance
64 Imaging (MRI) routinely provides a non-invasive method of assessing both function
65 and structure in live subjects. MRI is widely used for clinical assessment of
66 cardiovascular disease in humans, providing measurements such as myocardial
67 mass, ventricular volumes, stroke volume, ejection fraction (Epstein, 2007) and
68 even quantitative myocardial perfusion (Jerosch-Herold, 2010) and blood flow maps
69 (Markl M, 2007) . Applications of cardiovascular MRI to other vertebrates, such as
70 rodents, are predominately focussed on biomedical research using disease models.
71 This research has driven the development of specialised MRI systems optimised for
72 mice and rats. The data needed for an MR image generally needs to be acquired
73 over several separate acquisitions. For cardiac MRI where the heart is in continual
74 motion, the MRI scanner typically needs to be triggered/gated by an ECG signal
75 identifying the phase of the cardiac cycle. This is called prospective gating.

76

77 Although MRI has been used previously to acquire basic MRI images of spider
78 anatomy (Pohlmann et al., 2007) it has never been used to study the cardiac
79 function of spiders. Indeed, conventional prospective gating with its need for ECG
80 electrodes and respiration probes is not practical for spiders due to the difficulty of

81 attaching electrode pads or needles. However, the recent development of
82 retrospectively gated cardiac cine-MRI (RG-CINE-MRI) (Heijman et al., 2006) has
83 simplified cardiac MRI experiments by removing the need for ECG and respiratory
84 contact probes (Holmes 2008, 2009). Here we seek to demonstrate this technology
85 to acquire the first *in vivo* cardiac images of a spider heart and obtain quantitative
86 measures of cardiac function. The Theraphosidae family and *Grammostola* genus
87 were chosen as subjects, being a good fit in terms of physical size for existing
88 commercial rat cardiac MRI coils. In addition, possessing hearts of comparable size
89 to rodent hearts helps produce good quality MRI images for quantitative analysis.
90 However it should be noted that the cardiac method described here would be equally
91 applicable to smaller spiders, if an appropriately sized MRI coil was used (Merrifield
92 et al 2017) . With the advent of coil-on-a-chip technology, the size of MRI coils now
93 ranges from several tens of centimetres down to just 50microns diameter (Webb
94 2013).

95

96 RG-CINE-MRI

97 **Materials and Method**

98

99 *Animal Ethics*

100

101 Experiments were conducted according to UK legislation (UK Animals (Scientific
102 Procedures) Act (1986)). Subjects were anaesthetised throughout scanning for
103 immobilisation and to reduce potential subject stress. Efforts were made to avoid
104 direct handling of subjects.

105

106 *Animal Details and Housing*

107

108 Six captive bred adult spiders (gender undetermined, exact age unknown but of adult
109 size, n = 4 *Grammostola rosea* (Walckenaer), n = 2 *Grammostola porteri* (Mello-
110 *Leitao*), Mean Mass = 15.7 g \pm 1.75) were obtained from a UK-based supplier
111 (Virginia Cheeseman, High Wycombe, UK). Spiders were individually housed in
112 plastic vivariums (Length = 29 cm, Width = 19 cm, Height = 23 cm). Sterilised
113 vermiculite substrate was provided (~4 cm deep) along with a retreat. A one week
114 acclimatisation period followed delivery of spiders before subsequent scanning. Free

115 access to water was provided. Food was withheld until after full recovery from
116 scanning and anaesthesia.

117

118 *Animal Anaesthesia, Handling and Positioning*

119

120 Following standard procedures in animal MRI research, subjects were anaesthetised
121 using 5% isoflurane delivered in a 30%/70% mixture of O₂/N₂O gas (1000 ml min⁻¹)
122 to minimise subject motion derived imaging artefacts (Fig 1B). Under anaesthesia all
123 measurements would also be taken at a physiological baseline, eliminating variation
124 due to involuntary movement or behaviour.

125

126 Subjects were positioned in an MRI compatible animal cradle, lying supine with the
127 heart close to the MRI coil (Fig. 1C). Restraints were cushioned by folded medical
128 gauze swabs that were placed along the length and width of the spider. The
129 assembly was then enclosed in a sealed clear plastic chamber to allow maintenance
130 of anaesthesia and for visual observation of the subject (Fig. 1D). This was then
131 placed into the MRI scanner.

132

133 After scanning was complete (>1 hour) subjects were in an unresponsive state
134 suggesting deep anaesthesia had been achieved. Locator scans performed before
135 and after cardiac scanning confirmed animals had remained in position during the
136 scanning procedure. Activity returned to normal over a subsequent 24-48 hour
137 period. After recovery no adverse health effects or anomalous behaviours were
138 noted.

139

140 *MRI Scanning*

141

142 Animals were scanned in a 7T Bruker Biospec MRI scanner (Figure 1A) equipped
143 with a 400 mTm⁻¹ gradient insert and 4-channel phased array cardiac coil (Rapid
144 Biomedical GmbH, Germany). Ambient room temperature during scanning was 18-
145 21°C. The animal was not directly heated by any additional equipment in this time.

146

147 Anatomical MRI scans were obtained to set up imaging slice prescriptions for Fast
148 Low Angle Shot (FLASH) based retrospective RG-CINE-MRI scans (repetition time

149 $T_R = 8.00\text{ms}$, echo time $T_E = 3.30\text{ms}$, field of view (FOV) = $30.0\text{mm} \times 30.0\text{mm}$,
150 matrix = 256×256 , in-plane resolution $117\mu\text{m} \times 117\mu\text{m}$, slice thickness = 1.50mm ,
151 14-18 slices depending on size of individual spider, 300 continuous k-space
152 acquisitions, 5mins 7secs imaging time per slice). These were obtained using an in-
153 slice navigator echo as part of the Intradate software package on the scanner
154 (Paravision v.4, Bruker). This navigator is used retrospectively to determine the
155 phase of the cardiac cycle associated with each k space acquisition, allowing images
156 to be created for 10 different phases of the cardiac cycle [Heijman et al., 2006;
157 Bovens SM et al., 2011]. Axial image slices along the length of the heart were
158 obtained sequentially until the whole heart was scanned marked by the distal and
159 proximal aortas.

160

161 *Image Reconstruction and Analysis*

162

163 Cardiac images were reconstructed using the software tools available in Bruker's
164 Intradate software. Residual navigator pulse trace discontinuities were excluded.
165 Heart rates for each acquired slice were individually outputted as part of this
166 process. Images were analysed using Image J (Schneider et al., 2012). Three
167 independent researchers were trained in cardiac image analysis and then each
168 conducted a separate analysis of all images. Researchers were blinded to which
169 subjects the images came from.

170

171 For each slice, images were acquired for 10 different phases of the cardiac cycle.
172 From the 10 images of the cardiac cycle for the central chamber, the images
173 corresponding to the diastolic and systolic phases were identified. For each slice at
174 diastole and systole, a region of interest was manually drawn around the heart
175 perimeter giving the area of the ventricle at diastole and systole. This area is then
176 converted to a volume for that slice by multiplying by the image slice thickness of
177 1.5mm . The total ventricular volume of the heart, the end diastolic volume (EDV) and
178 end systolic volume (ESV) are then given by summing the volumes from each slice.
179 The cardiac ejection fraction (EJ) was then determined by,

180

$$181 \quad EJ = \frac{(EDV - ESV)}{EDV}$$

182 . Calculations of global heart parameters were then made from these measurements.

183

184

185

186 Statistical Analysis

187

188 Where group averages are given they are presented with plus/minus the standard
189 deviation. In Figure 3a the error bars represent the range of values of the
190 measurement made by the three independent researchers. Researchers were
191 blinded to which spider the images had come from and slice ordering was
192 randomised for each researcher. From the RG-CINE-MRI navigator signal a heart
193 rate is measured for each of the (14 to 18) slices acquired. The heart rate was then
194 presented as the mean and standard deviation of these values (figure 3b).
195 Correlations were performed using Pearson correlation coefficient and a 2-tailed test
196 of significance (OriginPro 8, OriginLab Corporation).

197

198

199

200 Results

201

202 Cardiac Anatomy

203

204 Scans revealed anatomy matching that broadly outlined for spiders in existing
205 literature (Paul et al. 1994, Foelix 1996, Huckstorf K 2013). Figures 2a and 2b show
206 typical image slices acquired from the RG-CINE-MRI scans. Figure 2c shows a set
207 of ostia in the open position as the heart chamber fills with blood. Figure 2d shows
208 the same slice but with the heart now filled and the ostia closed. Blood pooling
209 between the myocardium and pericardium prior to injection to the interior of the
210 myocardium was also visible.

211

212 Heart Rate

213

214 Resting heart rates were measured via the RG-CINE-MRI technique as outputted by
215 navigator signal data. Multiple samplings on each spider were yielded by measuring

216 the heart rate in each image slice. The mean heart rate for the group of spiders was
217 20 bpm \pm 2 and showed good consistency between subjects using this method (Fig.
218 3B). No significant correlation was found between body mass and heart rate
219 (Pearson correlation -0.256, $p=0.62$).

220

221 Cardiac function

222

223 Table 1 shows quantitative measurements of cardiac function derived from the RG-
224 CINE-MRI datasets for each spider. As may be expected there was a significant
225 correlation between body mass and total heart volume (Pearson correlation 0.882,
226 $p=0.02$) and between body mass and end diastolic ventricular volume (EDV)
227 (Pearson correlation 0.956, $p= 0.006$). The fraction of blood ejected from the heart
228 with each heart beat (the cardiac ejection fraction (EJ)) was successfully measured
229 in each spider as a measure of cardiac function (Fig. 3A). These are the first
230 measurements of *in vivo* ejection fraction in spiders that we were able to find in the
231 literature. Interestingly, we find a significant correlation between body mass and EJ
232 (Pearson correlation 0.849, $p= 0.03$). The difference in measurement of EJ between
233 the three researchers gave a mean observer difference of EJ = 5.9%. This mirrors
234 accepted levels of observer variability in corresponding rodent cardiac MRI (Heijman
235 et al., 2008). The motion of the heart over the full cardiac cycle at different positions
236 along the axis of the heart can clearly be seen in Supplementary Information 1-3.

237

238 Discussion

239

240 The spider heart differs in many structural and biochemical aspects to those of
241 vertebrates previously studied with MRI. However, the spider's contiguous nested
242 two chamber system - the heart myocardium surrounded by a pericardium (Paul et
243 al., 1994; Huckstorf et al., 2013) - provides a resultant MRI image similar to that of a
244 standard human/rodent short-axis view (Figure 2). Hence we used similar image
245 analysis methods to quantify cardiac function.

246

247

248 As might be expected we found a significant positive correlation between body mass
249 and both heart volume and ventricular volume. However, we also found a significant

250 positive correlation between body mass and ejection fraction. This is interesting as
251 in humans there is no significant correlation between body mass and ejection
252 fraction (Dorbala S. et al., 2006; Seo J. et al., 2017), but there is some correlation
253 between age and ejection fraction (Gebhard C. et al., 2012). A possible explanation
254 for this is that as spiders grow by iterative stages of moulting, a spider's mass can
255 serve as an approximate proxy for age (Foelix 1996). Therefore the correlation
256 observed between EJ and mass can also be broadly considered to be one of EJ and
257 age.

258

259 While the cardiac ventricular volume and to a lesser extent the total heart volume
260 changes between diastolic and systolic phases of the cardiac cycle as expected, the
261 total volume of the myocardial tissue remains largely unchanged in each spider and
262 between systolic and diastolic phases of the cardiac cycle. This suggests that the
263 material is being expanded and compressed across the cardiac cycle as would be
264 expected. No obvious trend for increase in myocardial material over animal mass
265 was observed in contrast to the trend observed for ventricular ejection fraction.

266

267 It can be speculated that if the growth of the heart volume and/or myocardial tissue
268 from one moulting instar to the next is less than that of the overall animal's volume
269 then a corresponding increase in EJ would be required. This means that the heart
270 would have to pump a larger volume of blood as it aged in order to maintain
271 adequate cardiac function, just as we observed. Further assessment of spiders of
272 different masses (and so at different ages or developmental instars at least) would
273 provide a more complete understanding of this relationship as well as potentially
274 revealing any additional physiological costs of this increased output as subjects age.
275 These costs might mirror mechanical heart degradation and disease in vertebrate
276 animals but could be of novel interest to cardiac researchers given the evolutionary
277 independent nature of the spider cardiac system as an invertebrate. Additionally, if
278 measurements of the mechanical properties of the spider heart could be conducted
279 *ex vivo*, then it would be possible to combine these with MRI to calculate the
280 biomechanical forces at work in the spider heart *in vivo*. Spider growth gradually
281 tapers off both physically and with frequency dependent on species, age and food
282 availability (Foelix 1996). It is conceivable that the end point to this process might be
283 marked or triggered by the condition of the heart, precluding further growth when

284 specific mechanical limits have been reached. The MRI technique we have
285 demonstrated here would be suitable for investigating this further.

286

287 The consistency of mean heart rate across subjects supports the use of non-contact
288 methods to assess heart function in spiders. Although some reports suggest that
289 heart rate across all spider species is correlated with animal mass (Carrel and
290 Heathcote 1976) this was not found to be the case for the subjects involved in our
291 study. However, the Carrel and Heathcote study treats multiple spider types in a
292 collective fashion, combining measurements from them all into a single trend for
293 heart rate and mass. This is despite known differences between these spiders in
294 terms of behaviour, environmental conditioning and physiology. This variation
295 between types is visible in the Carrel and Heathcote study itself. Our study suggests
296 that within groupings of spider type heart rate does not vary - certainly within the
297 Theraphosidae species. Comparative study of different types of spiders using MRI
298 would clarify this situation further.

299

300 A wider range of heart rate values was observed in two subjects in this study. These
301 two animals were scanned first. This greater range of obtained heart rates could be
302 explained by a poorer quality Intragate navigator signal resulting from increased
303 animal motion. In turn this could be due to less restrictive restraints used on these
304 initial two subjects as we finalised the experimental set up. However, mean values
305 are still acceptably consistent with those found in the subsequent scanned subjects.

306

307 We were unable to absolutely determine the gender of the subjects scanned, but
308 their large size (indicating greater age) and continued life-span post-scanning (years)
309 suggests they were all female. This would also tally with the assessment of the
310 supplier. It is possible that our group of subjects included a mix of both male and
311 female subjects which may have resulted in some of the variation in results.
312 However, sexing of spiders is notoriously difficult until males reach sexual maturity in
313 the final instar of growth and so may continue to be difficult to determine.

314

315 Despite reports of the effectiveness of isoflurane-based inhalation anaesthesia
316 induction in spiders (Zachariah et al., 2009; Dombrowski et al., 2013) we found it to
317 have variable performance (Pizzi 2012). Some spiders were rendered lethargic after

318 5-10 minutes. In others it appeared to have minimal effect even for induction times
319 greater than 30 minutes. The brief time needed to move the animal from the
320 induction chamber to the scanning chamber (<15 seconds) was often sufficient for
321 recovery from the initial lethargic state.

322

323 Although alternative injectable anaesthetics have been studied recently in spiders
324 (Gjeltema 2014) more effective inhalation anaesthesia agents should be investigated
325 for future use. Additionally, the design and use of a combined induction/scanning
326 chamber is recommended to avoid the need to remove spiders from the anaesthesia
327 environment. Placement of the spiders in an oxygen enriched environment post-
328 scanning is recommended to potentially accelerate recovery from the deep level of
329 anaesthesia induced in subjects over the scan duration.

330

331

332 The RG-CINE-MRI sequence used was designed for rodent hearts beating at much
333 higher rates compared to spiders (~20 beats per minute (bpm) compared to
334 ~350bpm in rats and ~550 bpm in mice). Therefore, a potential concern was that the
335 spider heart rate would be insufficient and provide too few complete cardiac cycles
336 for the reconstruction algorithms of the RG-CINE-MRI software to work. This did not
337 prove as problematic as originally thought and the reconstruction appeared robust
338 and consistent with experience in house.. Our own particular scan settings may not
339 be optimal in terms of balancing total scan time (and so cost) against the obvious
340 benefits of *in vivo* MRI as a technique. Fewer image averages and Intragate cardiac
341 cycles should be possible to speed up the imaging process without compromising
342 the final measurement quality. Our high imaging resolution enabled us to see the
343 operation of the heart ostia, but for simple analysis of heart function the image
344 resolution could also be reduced, speeding up image acquisition further. It should be
345 noted that in these experiments the RG-CINE-MRI for each slice was acquired
346 sequentially. We found this gave stable pseudo cardiac and respiratory gating
347 signals that are needed for the retrospective reconstruction of the cardiac images.
348 However, a more efficient multi-slice approach is often used in rodent cardiac
349 studies, which could be potentially applied to spiders (Heijman et al., 2006).

350

351 These results suggest that RG-CINE-MRI can potentially be applied to spiders and

352 other invertebrates. The availability of MRI micro-coils, from just 50um diameter
353 (Webb 2013), would allow even small invertebrates to be studied. However, it is
354 worth noting that the centralised, cohesive heart structure of spiders is comparatively
355 rare. Amongst both arachnids and insects, a chain of small 'pseudo-hearts' that act
356 collectively is more the norm (Klowden 2007). Though, the application of RG-CINE-
357 MRI to such a chain of pseudo hearts should be technically possible, it would need
358 to be practically tested.

359

360 In summary, we acquired the first *in vivo* cinematic cardiac MRI images from spiders.
361 From these images we were able to directly measure common cardiac functional
362 parameters for the first time in an identical manner to existing human and rodent
363 cardiac MRI. Cardiac ejection fraction was found to increase with animal mass at a
364 faster rate than myocardial tissue volume while heart rate stayed constant across
365 animals, suggesting the spider heart undergoes additional biomechanical loading
366 with age. The RG-CINE-MRI technique provides much potential for *in vivo* cardiac
367 MRI research to be expanded into a wider range of novel species.

368

369 **Acknowledgements**

370

371 The authors thank Dr M. A. Jansen and Prof. W. N. McDicken for advice throughout
372 this project.

373

374 **Supporting Information**

375 Additional Supporting Information may be found in the online version of this article.

376 Movie M1 Example CINE cardiac movie

377 Movie M2 Example CINE cardiac Movie

378 Movie M3 Example CINE cardiac Movie

379

380 **Contributions**

381

382 GM and WMH conceived and designed the experiments. GM, JM, LG, RP and WMH
383 performed the experiments. GM, NB and LH analysed the resultant images and data.

384 GM, NB and WMH prepared the manuscript

385

386

387 **References**

388

389 **Bromhall C.** (1987). Spider heart-rates and locomotion. *Journal of Comparative*
390 *Physiology B* **157**, 451-460.

391

392 **Bovens S.M., Boekhorst B.C.M.T., den Ouden K., van de Kolk K.W.A., Nauerth**
393 **A., Nederhoff M.G.J., Pasterkamp G., ten Hove M., van Echteld C.J.A.** (2011)
394 Evaluation of infarcted murine heart function: comparison of prospectively triggered
395 with self-gated MRI. *NMR in Biomedicine*. **24**, 307-315.

396

397 **Carrel J.E. and Heathcote R.D.** (1976) Heart Rate in Spiders: Influence of Body
398 Size and Foraging Energetics. *Science, New Series*, **193**, 148-150.

399

400 **Coelho F.C. and Amaya C.C.** (2000). Measuring the heart rate of the spider,
401 *Aphonopelma hentzi*: a non-invasive technique . *Physiological Entomology*, **25**, 167–
402 171. (doi:10.1046/j.1365-3032.2000.00182.x)

403

404 **Dombrowski, D.S., De Voe R.S. and Lewbart G.A.** (2013) Comparison of
405 Isoflurane and Carbon Dioxide Anesthesia in Chilean Rose Tarantulas (*Grammostola*
406 *rosea*). *Zoo Biol.* **32**, 101–103. (doi: 10.1002/zoo.21026)

407

408 **Dorbala S., Crugnale S., Yang D., Di Carli M.F.** (2006). Effect of body mass index
409 on left ventricular cavity size and ejection fraction. *American Journal of Cardiology*
410 **97**, 725-729

411

412 **Dunlop J.A., Altringham J.D. and Mill P.J.** (1992). Coupling between the heart and
413 sucking stomach during ingestion in a tarantula. *J. Exp. Biol.* **166**, 83-93.

414

415 **Epstein F.H.** (2007). MRI of left ventricular function. *Journal of Nuclear Cardiology.*
416 **40**, 729-744.

417

418 **Foelix R.F.** (1996) *Biology of Spiders*. Oxford, UK; Oxford University Press.

419

420 **Gebhard C., Staehli, B. E, Gebhard, C. E., Jenni, R.,Tanner, F. C.** (2012). Effect of
421 age on left ventricular ejection fraction assessed by echocardiography. *European*
422 *Heart Journal*, 33, 565-565

423

424 **Gjeltema J., Posner L.P., and Stoskopf M.** (2014). The use of injectable
425 alphaxalone as a single agent and in combination with ketamine, xylazine, and
426 morphine in the Chilean rose tarantula, *Grammostola rosea*. *Journal of Zoo and*
427 *Wildlife Medicine* 45(4):792-801. 2014 (doi: <http://dx.doi.org/10.1638/2013-0223.1>)

428

429

430 **Heijman E., de Graaf W., Niessen P., Nauerth A., van Eys G., de Graaf L.,**
431 **Nicolay K. and Strijkers G.J.** (2006). Comparison between prospective and
432 retrospective triggering for mouse cardiac MRI. *NMR in Biomedicine* **20**, 439447
433 (doi:10.1002/nbm.1110)

434

435 **Heijman E., Aben J.P., Penners C. et al.** (2008). Evaluation of manual and
436 automatic segmentation of the mouse heart from CINE MR images. *Journal of*
437 *Magnetic Resonance Imaging* **27**, 86-93. (doi:10.1002/jmri.21236)

438

439 **Holmes W.M., McCabe C., Mullin J.M., Condon B., Bain M.M.** (2008) Non-
440 Invasive Self-Gated MR Cardiac Imaging of Developing Chick Embryos In-Ovo.
441 *Circulation*. 117, E346-347.

442

443 **Holmes W.M., McCabe C., Mullin J.M., Condon B., Bain M.M.** (2009). In ovo non-
444 invasive quantification of the myocardial function and mass of chick embryos using
445 magnetic resonance imaging. *NMR in Biomedicine*. 22: 745-752.

446

447 **Huckstorf K., Kosok G., Seyfarth E.A., Wirkner C.S.** (2013). The hemolymph
448 vascular system in *Cupiennius salei* (Araneae: Ctenidae), *Zoologischer Anzeiger*
449 **252**, 76-87. (doi:10.1016/j.jcz.2012.03.004)

450

451 **Jerosch-Herold M.** (2010). Quantification of myocardial perfusion by cardiovascular
452 magnetic resonance. *Journal of Cardiovascular Magnetic Resoance*. 12, 57.

453

454 **Klowden M.J.** (2007) *Physiological Systems in Insects*. Burlington, USA; Academic
455 Press.
456

457 **Markl M., Frydrychowicz A., Kozerke S.** (2007). 4D Flow MRI. *Journal of Magnetic*
458 *Resonance Imaging*. 36, 1015-1036.
459

460 **Merrifield G.D., Mullin J., Gallagher L., Tucker C., Jansen M.A., Denvir M.,**
461 **Holmes W.M.** (2017). Rapid and recoverable *in vivo* MRI of adult zebrafish at 7T.
462 *Magnetic Resonance Imaging*. **37**, 9-15.
463

464

465 **Paul R.J., Bihlmayer S., Colmorgen M. and Zahler S.** (1994). The Open
466 Circulatory System of Spiders (*Eurypelma californicum*, *Pholcus phalangioides*): A
467 Survey of Functional Morphology and Physiology. *Physiological Zoology* **67**, 1360-
468 1382.
469

470 **Pizzi, R.** (2012). Spiders. In: *Invertebrate Medicine*, 2nd edition (ed Lewbert, G.A.)
471 pp. 187-222, Chichester, UK; Blackwell Publishing
472

473 **Pohlmann A., Möller M., Decker H., and Schreiber W.G.** (2007). MRI of tarantulas:
474 morphological and perfusion imaging. *Magn Reson Imaging*. **25**, 129-35.
475

476 **Seo J.S., Jin H.Y., Jang J.S., Yang T.H., Kim D.K., Kim D.S.** (2017). The
477 Relationships between Body Mass Index and Left Ventricular Diastolic Function in a
478 Structurally Normal Heart with Normal Ejection Fraction. *J Cardiovasc Ultrasound*.
479 **25**, 5-11
480

481 **Schneider C.A., Rasband W.S. and Eliceiri K.W.** (2012). NIH Image to ImageJ: 25
482 years of image analysis. *Nature Methods* **9**, 671-675.
483

484 **Webb A.G.** (2013). Radiofrequency microcoils for magnetic resonance imaging and
485 spectroscopy. *Journal of Magnetic Resonance*. 229, 55-66.
486

487 **Zachariah T.T., Mitchell M.A., Guichard C.M. and Singh R.S.** (2009). Isoflurane

488 anesthesia of wild-caught goliath birdeater spiders (*Theraphosa blondi*) and Chilean
 489 rose spiders (*Grammostola rosea*). *J Zoo Wildl Med* **40**, 347–349.
 490
 491

Spider	1	2	3	4	5	6	Mean \pm std
Body Mass (g)	11.7	12.00	12.00	15.10	16.09	18.8	14 \pm 3
Heart Rate (beats/min)	20.2 (± 1)	20.6 (± 1)	21.1 (± 2)	22.9 (± 4)	16.0 (± 3)	20.6 (± 6)	20 \pm 2
End systolic ventricular Volume (ESV) (mm ³)	29.6	50.0	30.7	28.6	53.7	49.4	40 \pm 12
End Diastolic ventricular Volume (EDV) (mm ³)	42.5	57.5	51.1	59.9	96.5	115.1	70 \pm 29
Ejection Fraction (EJ)	0.25 (± 0.04)	0.13 (± 0.02)	0.37 (± 0.04)	0.52 (± 0.02)	0.48 (± 0.04)	0.57 (± 0.01)	0.38 \pm 0.17
Heart volume (systole) (mm ³)	114	134	91.8	135	176	184	139 \pm 35
Heart volume (diastole) (mm ³)	122	140	114	170	213	232	165 \pm 48
Volume of Myocardium (systole) (mm ³)	84.0	83.7	61.1	106	123	135	99 \pm 28
Volume of Myocardium (diastole) (mm ³)	79.3	82.6	63.1	110	116	117	95 \pm 23
Change in myocardium Thickness (mm ³)	0.06	0.01	-0.02	-0.03	0.08	0.15	0.04 \pm 0.07

492 Table 1. Cardiovascular physiological measurements made on each of the six
 493 spiders from the cine MRI datasets. The mean values from all six spiders is given in
 494 the end column

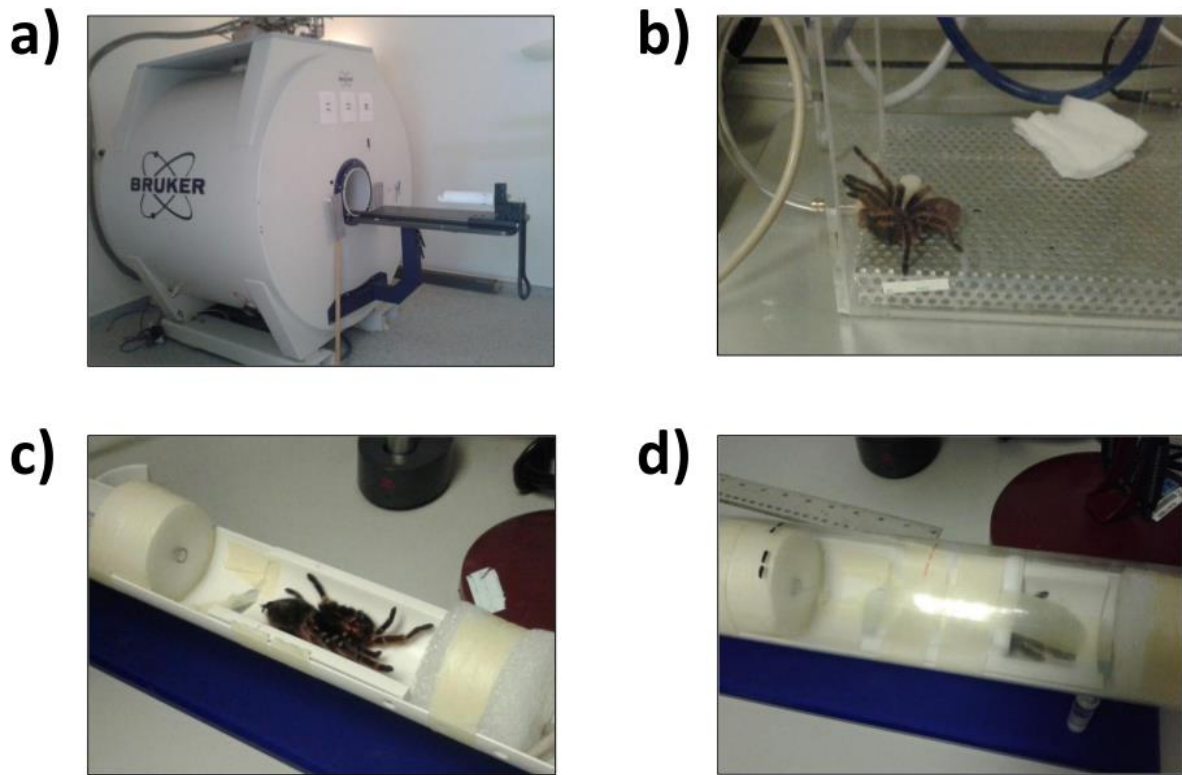
495
 496
 497
 498

499 **Figure Legends**

500
 501

502 **Figure 1. Experimental set up for scanning. A.** 7T preclinical MRI scanner used in
 503 the experiments, **B.** Spider in anaesthetic chamber undergoing anaesthesia

504 induction, **C.** Anaesthetised spider lying prone on back in place above MRI coil, **D.**
505 Spider ready for scanning now with restraints in place and with plastic sleeve in
506 place over the coil and cradle.

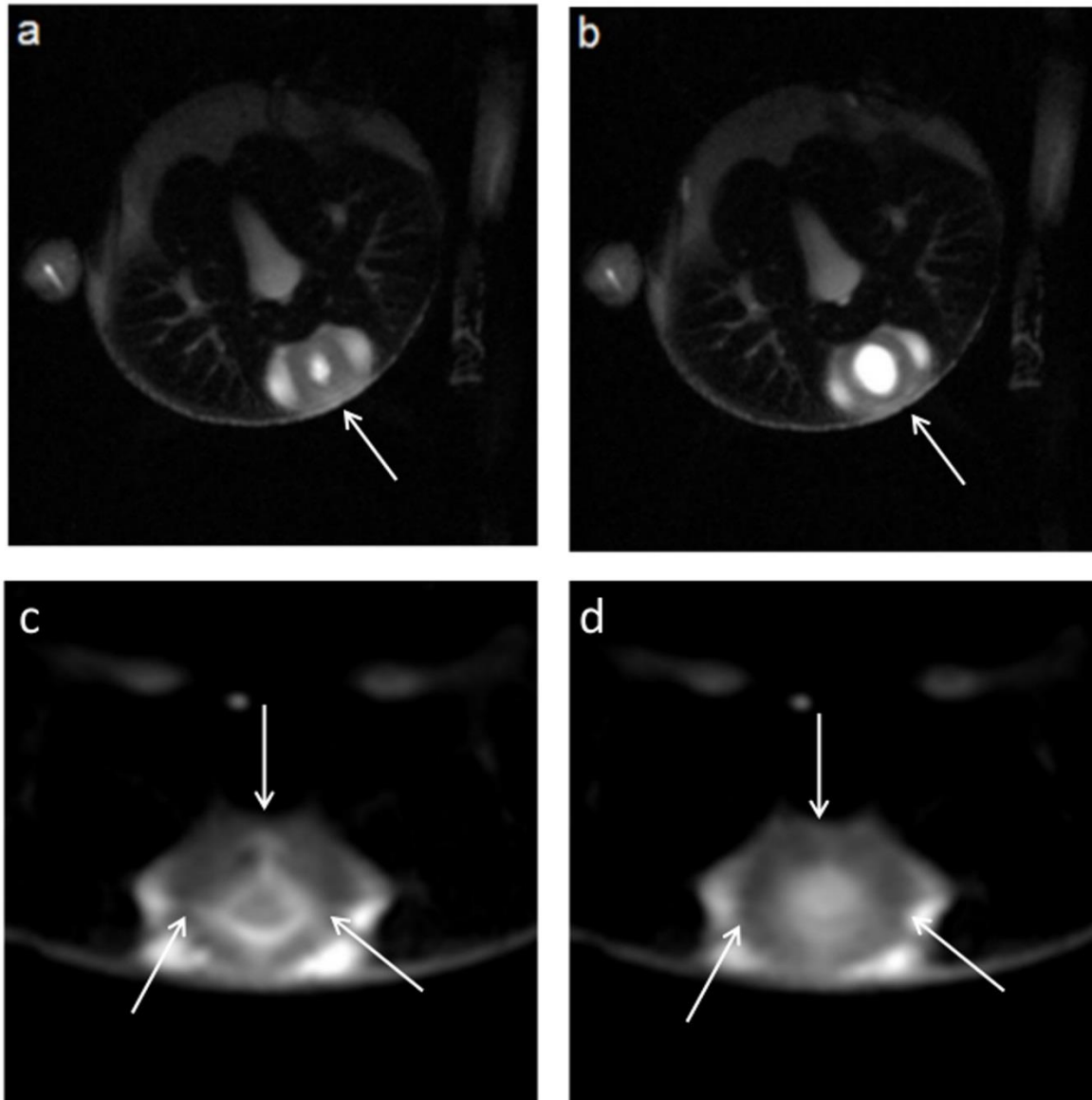


507

508

509

510 **Figure 2. Example cardiac images from RG-CINE-MRI data.** Axial image slices
511 showing **A.** Diastolic phase (heart arrowed), **B.** Systolic phase (heart arrowed), **C.**
512 Heart with ostia (arrowed) in the open position, **D.** Heart with ostia (arrowed) in the
513 closed position.



514

515

516

517 **Figure 3. Results of Cardiac MRI Analysis showing A.** Mean and standard
518 deviation of measurements of cardiac ejection fraction determined between three
519 independent researchers (for n=6 spiders). **B.** RG-CINE-MRI navigator sourced
520 mean heart rates in Beats Per Minute (BPM) with s.d. error bars. After RG-CINE-MRI
521 navigator signal processing the mean heart rate for each slice of cardiac data from
522 an individual subject is estimated and then a mean heart rate is generated for the
523 entire heart (n=6).

